

# Unmasking the Annexin I Interaction from the Structure of Apo-S100A11

Anne C. Dempsey,<sup>1</sup> Michael P. Walsh,<sup>2</sup>  
and Gary S. Shaw<sup>1,\*</sup>

<sup>1</sup>Department of Biochemistry  
The University of Western Ontario  
London, Ontario N6A 5C1  
Canada

<sup>2</sup>Department of Biochemistry and Molecular  
Biology  
University of Calgary  
Calgary, Alberta T2N 4N1  
Canada

## Summary

S100A11 is a homodimeric EF-hand calcium binding protein that undergoes a calcium-induced conformational change and interacts with the phospholipid binding protein annexin I to coordinate membrane association. In this work, the solution structure of apo-S100A11 has been determined by NMR spectroscopy to uncover the details of its calcium-induced structural change. Apo-S100A11 forms a tight globular structure having a near antiparallel orientation of helices III and IV in calcium binding site II. Further, helices I and IV, and I and I', form a more closed arrangement than observed in other apo-S100 proteins. This helix arrangement in apo-S100A11 partially buries residues in helices I (P3, E11, A15), III (V55, R58, M59), and IV (A86, C87, S90) and the linker (A45, F46), which are required for interaction with annexin I in the calcium-bound state. In apo-S100A11, this results in a “masked” binding surface that prevents annexin I binding but is uncovered upon calcium binding.

## Introduction

The calcium ion acts as an important second messenger controlling integral cellular events such as neurotransmitter release, vision, and muscle contraction. In many cases, a member of the EF-hand family of calcium binding proteins plays an intermediary role in these processes through either calcium-dependent interactions with selected target proteins or maintenance of intracellular calcium levels. In the first mechanism, calcium binding to an EF-hand protein results in a significant conformational change in the protein and a change in its surface properties, facilitating the interaction with other proteins. The EF-hand proteins troponin-C and calmodulin are members of this category of “sensor” proteins (Ikura, 1996), having their respective interactions with troponin-I (McKay et al., 1997) and myosin light chain kinase (among others; Ikura et al., 1992) controlled by calcium binding.

Recently, three-dimensional structures of proteins in the S100 family of EF-hand proteins have indicated

some members of this family may act as calcium signaling or sensor proteins (Drohat et al., 1998; Maler et al., 2002; Otterbein et al., 2002; Sastry et al., 1998; Smith and Shaw, 1998b). The S100 proteins are small acidic proteins of approximately 10–12 kDa in molecular weight and found only in vertebrates. To date there have been nineteen S100 proteins identified, most of which appear to be cell specific (Donato, 2001; Heizmann, 1999; Heizmann et al., 2002). For example, S100B is concentrated in glial cells (Petrova et al., 2000), while S100P is located mainly in placental tissue (Becker et al., 1992). Several of the S100 proteins have also been linked with disease states such as Alzheimer's and rheumatoid arthritis, usually via the overexpression of the protein (Odink et al., 1987; Van Eldik and Griffin, 1994). However, the cause of the overexpression and details of the roles of these proteins in disease is still uncertain. Other S100 proteins have been shown to interact with a variety of proteins such as tubulin (Garbuglia et al., 1999), annexins I, II, and VI (Bianchi et al., 1992; Garbuglia et al., 1998; Gerke, 1990; Seemann et al., 1996), p53 (Baudier et al., 1992; Delphin et al., 1999), and actin (Fujii et al., 1990), and are proposed to regulate processes such as assembly, phosphorylation, and membrane interaction.

S100A11 (S100C, calgizzarin) is a member of the S100 family, which is often expressed in smooth muscle (Allen et al., 1996; Schönekeess and Walsh, 1997; Seemann et al., 1996). S100A11 has been shown to interact with the phospholipid binding protein annexin I in a calcium-sensitive manner (Seemann et al., 1996). In this mechanism, the N-terminal helix of annexin I is released from interaction with the third repeat in the annexin molecule (Gerke and Moss, 2002). This helix then associates with calcium-bound S100A11 where it could act as a bridge to link pairs of phospholipid-containing membranes. In the absence of calcium, annexin I has negligible affinity for S100A11 or the phospholipid matrix. Consistent with this role and an intracellular location near the interior of membranes, the calcium affinity for S100A11 is lower ( $K_d^{\text{Ca}} \sim 10^{-4}$  M) than that typically found for other S100 proteins ( $K_d^{\text{Ca}} \sim 10^{-5}$ – $10^{-6}$  M), because the local calcium concentration appears higher near the membrane. It is likely the affinity of S100A11 for calcium is increased in the presence of a target protein, as has been noted for calmodulin (Martin et al., 1996; Olwin and Storm, 1985; Yazawa et al., 1987). In support of this hypothesis, the affinity of S100A11 for calcium is enhanced  $\sim 10$ -fold in the presence of the hydrophobic probe 2-*p*-toluidinyl-naphthalene-6-sulfonate (Allen et al., 1996). Other studies have shown that S100A11 associates with F-actin, where it can inhibit its myosin  $\text{Mg}^{2+}$ -ATPase activity (Zhao et al., 2000).

S100A11, like most S100 proteins, is a dimeric protein, with each monomer comprising two helix-loop-helix motifs that coordinate the calcium ions. Calcium binding site I is comprised of helices I and II and a 14 residue “pseudo” calcium binding loop, while site II contains helices III and IV with a 12 residue canonical calcium binding loop. Calcium binding to most S100 proteins

\*Correspondence: [gshaw1@uwo.ca](mailto:gshaw1@uwo.ca)

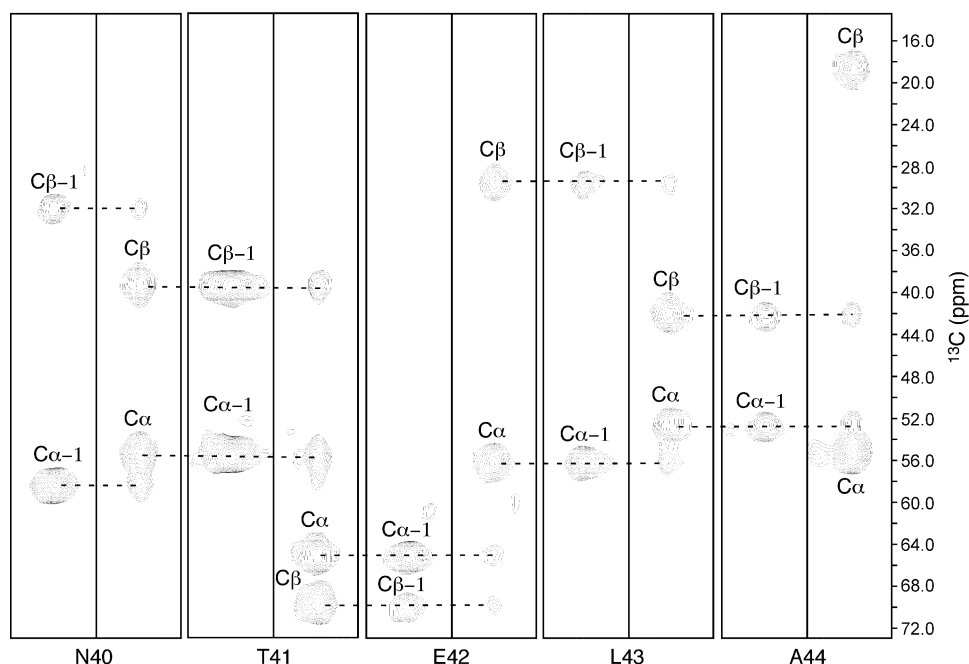


Figure 1. Selected Regions of 600 MHz NMR Spectra Used for the Backbone Assignment of Apo-S100A11

The spectra show  $^{15}\text{N}$  planes for the residues N40–A44 at the C terminus of helix II and start of the linker. For each pair of planes, the CBCA(CO)NH is shown on the left and the HNCACB is shown on the right. The  $\text{C}\alpha$  and  $\text{C}\beta$  for the indicated residue are shown on the HNCACB spectra and the corresponding  $\text{C}\alpha$  and  $\text{C}\beta$  for the previous ( $i - 1$ ) residue are shown in the CBCA(CO)NH. The spectrum was collected on a 1.0 mM apo-S100A11 sample in 90%  $\text{H}_2\text{O}/10\%$   $\text{D}_2\text{O}$  containing 50 mM KCl, 10 mM dithiothreitol (pH 7.25) at 35°C.

causes a significant reorientation of one or more of the helices, resulting in an exposure of hydrophobic residues previously buried in the apo-state (Maler et al., 2002; Smith and Shaw, 1998a). For example, calcium binding to human S100B triggers a reorientation of helix III with respect to helix IV and extends the  $\alpha$  helix in helix IV by one turn (Drohat et al., 1998; Matsumura et al., 1998; Smith and Shaw, 1998b). This results in the exposure of several hydrophobic residues in the C terminus and linker region of the protein, providing a surface for target interaction. In S100A6, calcium binding induces a less dramatic conformational change, although a hydrophobic surface is still exposed. In general, it is thought that differences in the hydrophobic surfaces between S100 proteins and the magnitude of the conformational change confer target specificity for a variety of different proteins.

Recently, the crystal structure of calcium-bound S100A11 in complex with an N-terminal peptide of annexin I has been determined (Rety et al., 2000). The structure shows that the annexin interface occurs through interactions with the linker and helices III and IV of one monomer, and helix I of the other monomer in S100A11. Thus, the annexin molecule “bridges” the two S100 monomers. This interaction is very different from the interactions of another S100 protein, S100B, with two of its targets, p53 (Rustandi et al., 2000) and a 12 residue synthetic peptide, TRTK-12 (McClintock and Shaw, 2003). In both of these cases, there are no interactions with helix I in S100B, and each target peptide interacts with only one monomer. In the calcium-bound S100A11/annexin I complex, interactions between S100A11 and annexin I

are facilitated by an open conformation of helices III and IV, which are near perpendicular to one another. Comparison to other apo-S100 protein structures suggests that these helices have reoriented upon calcium binding in order to create a hydrophobic cleft for target binding. However, the absence of an S100A11 structure in the calcium-free state and the differences from the calcium-bound S100B complexes makes the details of the conformational change and protein-protein interactions in S100A11 difficult to assess. In this work, we have determined the three-dimensional structure of rabbit apo-S100A11 by NMR spectroscopy in order to identify the conformational change that occurs in this protein and identify residues that confer specificity for target protein binding. The structure reveals that helices I and I' at the dimer interface of apo-S100A11 form a more closed arrangement compared to other apo-S100 proteins, while helices III and IV form a near antiparallel arrangement. This conformation of apo-S100A11 buries residues required for annexin I interaction found in helices I, III, and IV and the linker region. Upon calcium binding to S100A11, these residues are unmasked to reveal a stunning contiguous binding surface.

## Results and Discussion

The backbone and side chain resonance assignments for apo-S100A11 (Rintala et al., 2002) were determined by the collection and analysis of a set of two- and three-dimensional NMR experiments. The NMR spectra of apo-S100A11 were of high quality and well resolved. Figure 1 shows a strip plot of the CBCA(CO)NH and

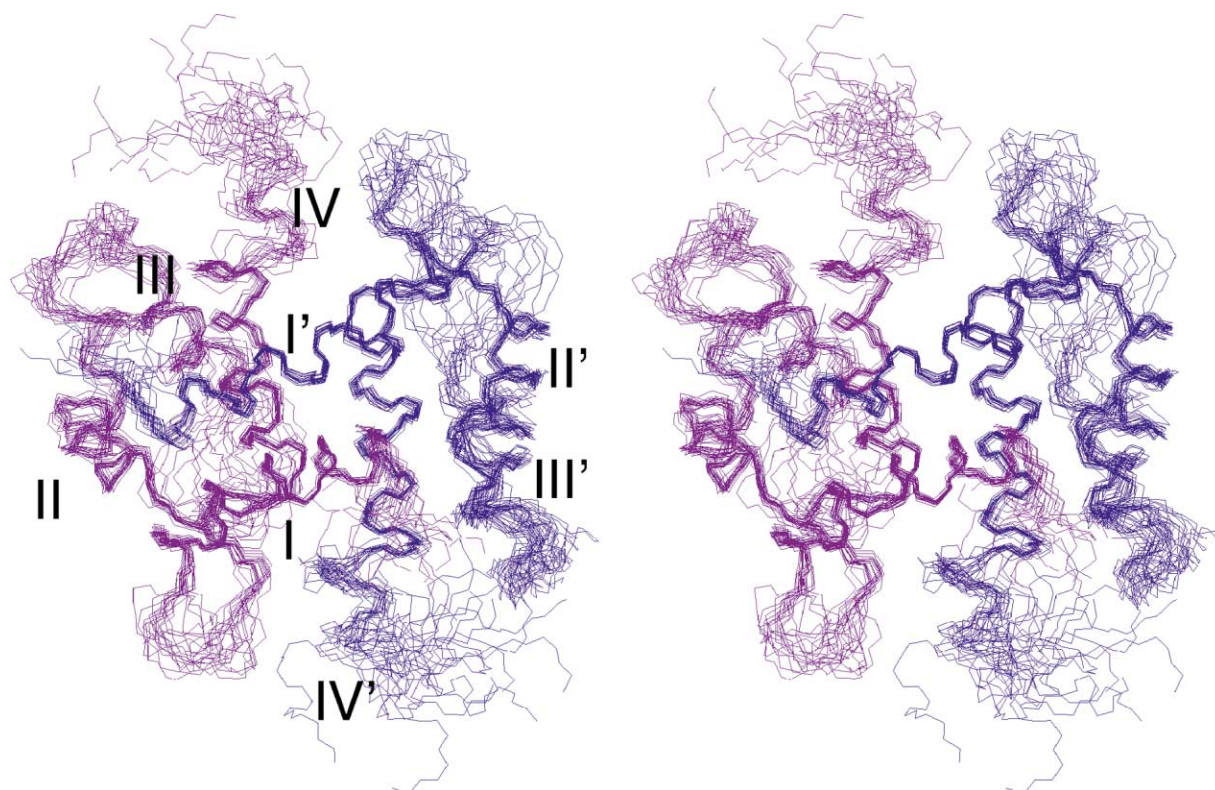


Figure 2. Structures of Apo-S100A11

Stereo view of the backbone superposition for the family of 19 low-energy structures of apo-S100A11 based on nOe, dihedral, and chemical shift NMR restraints. The two S100A11 monomers in the protein are colored magenta and blue to distinguish them. Helices are labeled I–IV in the first monomer and I'–IV' in the second. The superposition utilized the residues found in the regular secondary structure of the protein (eight helices; 5–20, 32–38, 56–60, and 74–85 and 5'–20', 32'–38', 56'–60', and 74'–85') and had an rmsd to the mean structure of  $0.45 \pm 0.08$  Å for backbone residues and  $1.15 \pm 0.21$  Å for all heavy atoms, respectively.

HNCACB spectra for several sequential residues (N40–A44) in the linker region of the protein. There were some difficulties assigning the backbone of the serine residues of the protein. To make their assignment possible, specifically  $^{15}\text{N}$ -glycine/serine-labeled S100A11 was prepared and a  $^1\text{H}$ - $^{15}\text{N}$  HSQC of those residues was collected and analyzed. This also facilitated the assignment of cysteine residues C9 and C87, because a small amount of transamination occurred during the labeling step. The chemical shifts for  $\text{C}\beta$  of these cysteine residues indicated the protein was in a fully reduced state. This observation is in contrast to that observed in the structure of calcium-bound S100A11 in complex with the annexin I peptide, where a C9–C9' intermolecular disulfide is present (Rety et al., 2000). Although apo-S100A11 also had a strong tendency to oxidize, this was suppressed using high quantities of dithiothreitol in all NMR samples. Stereo-specific assignment of the methyl groups of valine and leucine residues was achieved by the analysis of a  $^{13}\text{C}$ -coupled  $^1\text{H}$ - $^{13}\text{C}$  HSQC spectrum of fractionally  $^{13}\text{C}$ -labeled S100A11 (Neri et al., 1989). This method differentiates the *pro*-R methyl groups ( $\text{H}_{\gamma_1}$  or  $\text{H}_{\delta_1}$  of valine and leucine, respectively) from the *pro*-S methyl groups based on  $^{13}\text{C}$ - $^{13}\text{C}$  coupling. In apo-S100A11, all 5 valine and 11 leucine residues had stereo-specific assignments completed.

#### Description of the Structure of Apo-S100A11

A total of 3028 distance restraints and 192 dihedral restraints was used for the calculation of the three-dimensional structure of the apo-S100A11 dimer. Figure 2 shows a superposition of an ensemble of 19 structures of apo-S100A11. These structures were chosen based on their low energy and contained no distance violations greater than 0.5 Å and no angle violations greater than  $5^\circ$ . The family of structures shows the presence of four well-defined helices (I–IV) within each monomer. The rmsd of these regions in the dimer relative to the mean structure is  $0.45 \pm 0.08$  Å for the backbone and  $1.15 \pm 0.21$  Å for all heavy atoms. Each of the four helices is well defined (average  $0.20 \pm 0.08$  Å), with helix IV having the lowest rmsd ( $0.14 \pm 0.06$  Å), and helix II being the least well defined ( $0.23 \pm 0.10$  Å). A short antiparallel  $\beta$  sheet was identified within each monomer between residues T29 and S31 in calcium binding loop I, and residues Q70 and D72 in loop II. For this region, nOes were found across the  $\beta$  sheet between protons of T29 with L71 and D72, L30 with L71, and S31 with Q70. The extreme N terminus and the last 15 residues of the C terminus of apo-S100A11 are less well defined in the structures. This is likely a result of the lack of long-range nOes between S1–P3 and A86–F101, indicating these regions are flexible in solution. Further, chemical shift

Table 1. Structure Statistics for Apo-S100A11

Structure Statistics <sup>a</sup>	
Final Energies (kcal/mol)	
Total energy	159.42 ± 59.13
NOE energy	94.95 ± 7.71
Lennard-Jones VDW energy	-191.93 ± 45.57
Distance restraints > 0.5 Å	0
Angle violations > 5°	0
Rmsd from experimental distance restraints (Å)	0.0204 ± 0.0008
Rmsd from experimental angular restraints (Å)	0.5825 ± 0.0596
Restraints for Structural Calculations	
Total NOE Restraints	2964
Intraresidue	1336
Sequential	658
Short-range	594
Long-range	264
Intermolecular	112
Dihedral bond restraints	192
Hydrogen bonds	32
Ramachandran Plot	
Residues in favorable regions <sup>b</sup>	89.3%
Coordinate Precision <sup>c</sup>	
Rmsd to Mean (Å)	
Backbone atoms	0.45 ± 0.08
Heavy atoms	1.15 ± 0.21

<sup>a</sup>All statistics were calculated for a family of 19 structures.<sup>b</sup>This reflects residues in both most favored and additionally favored regions.<sup>c</sup>Precision is calculated for residues found in helices I (5–20), II (32–38), III (56–60), and IV (74–85) in apo-S100A11.

data were unable to find a consistent solution for  $\phi, \psi$  angles in these regions, indicating a range of angles is likely sampled for these residues. Table 1 shows the structural statistics for this family of structures. Analysis of this family of structures indicated that 89.3% of all of the residues are in the most favorable and additionally favorable regions of the Ramachandran plot.

The four helices in each S100A11 monomer were selected based on the superposition of structures and  $\phi, \psi$  angles from the Ramachandran plot and comprise helix I (E5–Y20), helix II (K32–F38), helix III (L56–M60), and helix IV (Q74–V85). The two  $\beta$  strands consist of the residues T29–S31 and Q70–D72 arranged in an antiparallel  $\beta$  sheet. Table 2 describes the interhelical angles of apo-S100A11. The arrangement of helices I and II for calcium binding site I in apo-S100A11 ( $\Omega = 116^\circ$ ) is most similar

to that observed for apo-S100A1 ( $\Omega = 120^\circ$ ) and apo-S100A4 ( $\Omega = 119^\circ$ ) (Rustandi et al., 2002; Vallely et al., 2002). Most interestingly, the interhelical angle between helices III and IV was found to be positive ( $\Omega = 154^\circ$ ) as in bovine apo-S100B ( $\Omega = 164^\circ$ ) (Kilby et al., 1996), apo-S100A6 ( $\Omega = 150^\circ$ ) (Maler et al., 1999; Otterbein et al., 2002; Potts et al., 1995), and apo-S100A4 ( $\Omega = 162^\circ$ ) (Vallely et al., 2002), while it has been found to be a negative orientation in rat apo-S100B (Drohat et al., 1999), apo-S100A1 (Rustandi et al., 2002), and apo-S100A3 (Fritz et al., 2002). This interaction in apo-S100A11 was supported by nOes from M59 to L79, M59 to L83, and M60 to L79. Together, these observations for calcium binding sites I and II indicate the helix interactions in apo-S100A11 are most reminiscent of apo-S100A4.

Dimerization of apo-S100A11 occurs through interac-

Table 2. Interhelical Angles<sup>a</sup> for Apo-S100A11 and Calcium-Bound S100A11/Annexin I Complex

Helix Pair	Apo-S100A11 <sup>b</sup>	S100A11-An I <sup>b,c</sup>	Difference <sup>d</sup>	Rmsd <sup>e</sup>
I-II	116 ± 3	129	13	1.00
I-III	-73 ± 5	-112	-39	1.62
I-IV	115 ± 2	127	12	1.18
II-III	159 ± 5	118	-41	1.38
II-IV	-41 ± 3	-29	12	1.49
III-IV	154 ± 3	115	-39	2.65
I-I'	-137 ± 3	-154	-17	-
IV-IV'	153 ± 5	153	0	-

<sup>a</sup>Determined using the program iha.1.4 (S. Gagné, Université Laval).<sup>b</sup>Helices were defined as residues 5–20, 32–38, 56–60, and 74–85 in apo-S100A11; 7–22, 34–40, 56–60, and 76–87 in the S100A11/annexin I complex.<sup>c</sup>Calcium-bound S100A11 in complex with the N-terminal helix from annexin I (Rety et al., 2000); PDB ID code 1QLS.<sup>d</sup>The difference reflects the change in interhelical angle between apo-S100A11 and the S100A11/annexin I complex. A positive number indicates a clockwise change and a negative number indicates a change in a counter-clockwise direction.<sup>e</sup>The backbone rmsd determined from a superposition of helices as defined in (b).

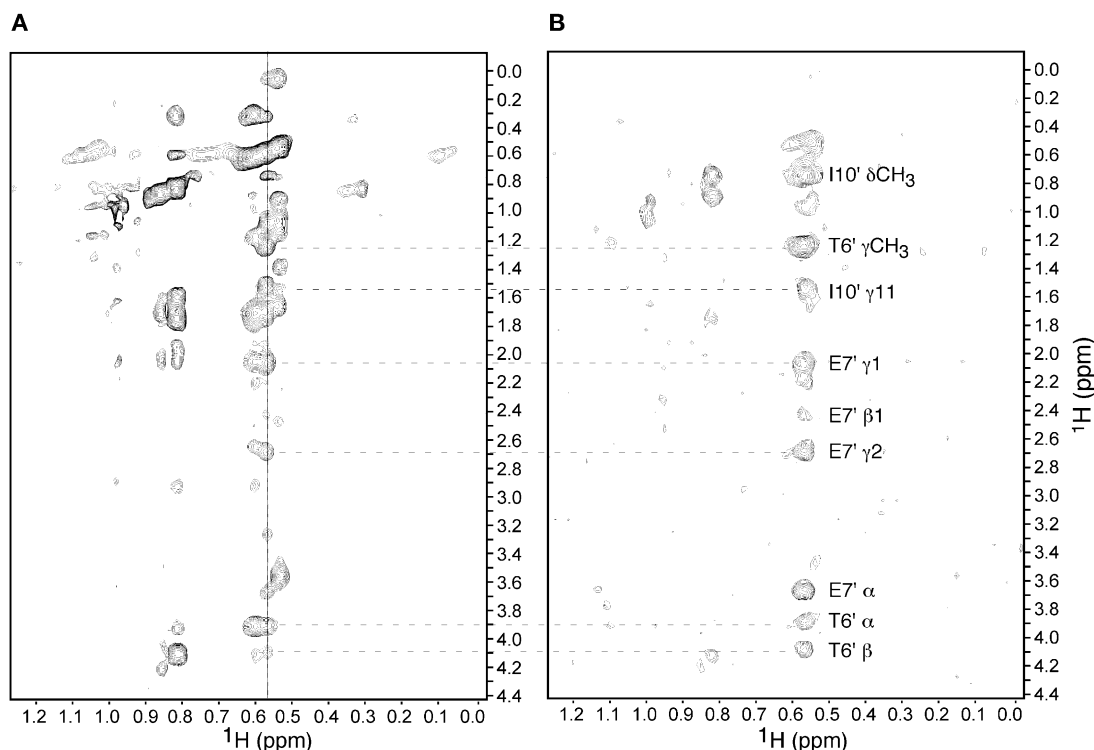


Figure 3. Identification of Residues at the Dimer Interface of Apo-S100A11

Regions of the  $^{13}\text{C},^{15}\text{N}$  NOESY (A) and  $^{13}\text{C}$  F<sub>1</sub>-filtered, F<sub>3</sub>-edited NOESY (B) showing the  $^{13}\text{C}$  plane at 23.95 ppm where L43  $\delta_2$   $\text{CH}_3$  is located at a  $^1\text{H}$  frequency of 0.56 ppm (shown in [A] by the vertical line). The  $^{13}\text{C},^{15}\text{N}$  NOESY (A) shows nOe crosspeaks from all protons whose attached  $^{13}\text{C}$  is found on this plane in apo-S100A11. The  $^{13}\text{C}$  F<sub>1</sub>-filtered, F<sub>3</sub>-edited NOESY spectrum (B) shows only those nOes (indicated by dashed lines) across the dimer interface involving L43  $\delta_2$   $\text{CH}_3$  from the linker on one monomer of apo-S100A11 and T6, E7, and I10 of helix I' of its partner monomer.

tions between helices I, I', IV, and IV', which form an X-type bundle. Specifically, the interhelical crossing angles for helices IV with IV' ( $153 \pm 5^\circ$ ) was similar to that observed in calcium-saturated S100A11 in complex with the annexin I peptide (Rety et al., 2000), while helices I and I' ( $137 \pm 3^\circ$ ) were more closed than in the complex ( $-154^\circ$ ). Residues that define the dimer interface for apo-S100A11 were identified from a  $^{13}\text{C}$  F<sub>1</sub>-filtered, F<sub>3</sub>-edited NOESY spectrum of the protein where one monomer was unlabeled and the other was  $^{13}\text{C},^{15}\text{N}$ -labeled. Figure 3 shows the  $^{13}\text{C}$  plane for L43  $\delta_2$   $\text{CH}_3$  (23.95 ppm) of the resulting  $^{13}\text{C}$  F<sub>1</sub>-filtered, F<sub>3</sub>-edited NOESY spectrum and the corresponding  $^{13}\text{C}$  plane of the  $^{13}\text{C},^{15}\text{N}$ -NOESY spectrum. The spectra show that residue L43 in the linker makes several contacts across the dimer interface with residues T6, E7, and I10 in helix I'. Other nOes from these data showed that T6 in helix I had close contacts with L13' and V16' in helix I', while C9 and I10 in helix I were close in space to L13'. Further, T6 and I10 in helix I had nOes with G80' and A84' in helix IV'. The helix IV-IV' interface was defined by nOes of F73 with G81', A84', and V85' as well as nOes from L77 to G80', G81', and A84'. These interactions aligned helices I and IV in opposite directions from helices I' and IV', respectively, in the dimer.

#### Apo-S100A11 Global Changes upon Complexation with Calcium and Annexin I

There have only been four three-dimensional structures of an S100 protein in complex with calcium and a target

protein (McClintock and Shaw, 2003; Rety et al., 1999, 2000; Rustandi et al., 2000). Of these, only S100B has structures available for the apo- (Drohat et al., 1999; Kilby et al., 1996), calcium- (Drohat et al., 1998; Matsuura et al., 1998; Smith and Shaw, 1998b), and target-bound states (McClintock and Shaw, 2003; Rustandi et al., 2000). For S100A11, a three-dimensional structure is available for the protein bound to the N-terminal region of the phospholipid binding protein, annexin I (Rety et al., 2000). Thus, the current structure of apo-S100A11 allows a comparison with the bound structure to determine regions that undergo a conformational change and are important for target protein recognition. Figure 4 shows a comparison of the structures of apo-S100A11 and the complex of calcium-bound S100A11 with an N-terminal peptide of annexin I. The structures reveal that every helix pair in S100A11, except that of helices IV and IV', shifts upon calcium binding and interaction with annexin I (Table 2). One of the most conservative changes in helix interaction involves helices I and II, which surround calcium binding site I. The interhelical angle for these helices is more open in the annexin complex by approximately  $13^\circ$ . Superposition of helices I and II from apo-S100A11 with those in the annexin complex reveals only a 1.00 Å rmsd between the two. This indicates that the conformation of site I is altered very little by calcium and/or annexin I binding. Similar observations have been made for S100B (Smith and Shaw, 1998b), S100A6 (Maler et al., 2002; Otterbein et



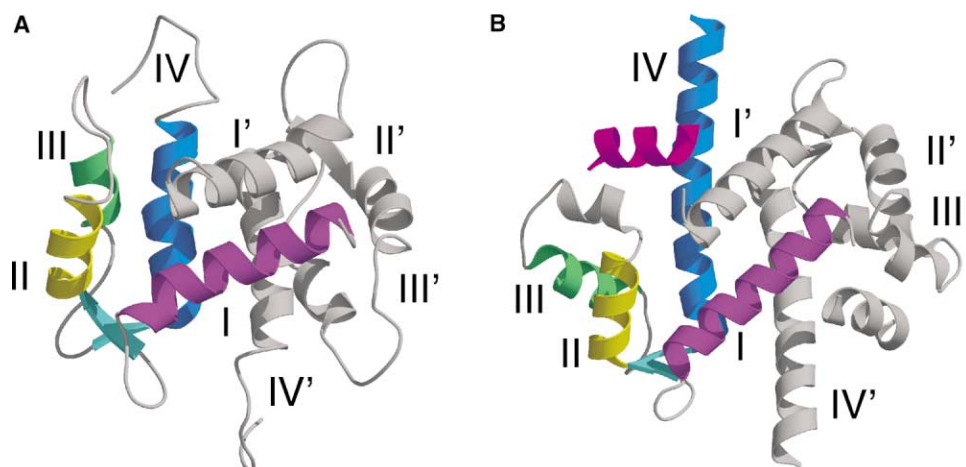


Figure 4. Global Conformational Change in S100A11

The ribbon diagrams of apo-S100A11 (A) and calcium-bound S100A11 (B) complexed to the N-terminal annexin I peptide (Rety et al., 2000) are shown in similar orientations. Although the structures are symmetric, only one monomer from each dimer is colored for easier viewing. For calcium-bound S100A11 (B), the annexin I peptide (magenta) interacts with helices III and IV and the linker of one monomer and helix I' of the partner monomer. The structures show that the orientations of helices I (purple) and II (yellow) in site I are similar upon calcium binding and complex formation. Helix I has shifted by approximately 17°, opening up the helix I-IV interhelical interaction. Helix III is nearly parallel ( $\Omega = 154 \pm 4^\circ$ ) to helix IV in apo-S100A11 and is almost perpendicular ( $\Omega = 115^\circ$ ) in the calcium-bound structure. Helix IV is notably shorter in apo-S100A11, ending near residue A85, whereas this helix is 10 residues longer in the annexin I complex. The calcium-bound S100A11 structure also contains a short helix in the linker region (gray) found in some structures of apo-S100A11.

al., 2002; Sastry et al., 1998), and calbindin D<sub>9k</sub> (Akke et al., 1992; Kordel et al., 1993; Skelton et al., 1995; Wimberly et al., 1995), which all possess a similar 14 residue pseudo-EF-hand calcium binding site I and is consistent with this loop being in a “calcium-ready” state.

Whereas the helix I-II interaction in apo-S100A11 appears largely conserved upon calcium binding, it is clear that the relationship of helix II to helices III and IV is altered. This is not obvious from the small interhelical angle shift between helices II and IV, which only differs by 12° in the two structures (Table 2) but is manifested in a larger rmsd between the helix pairs of 1.49 Å. A detailed analysis of S100A6 has revealed that similar changes in the helix II position result from the repacking of several residues in this helix upon calcium binding (Maler et al., 2002). Indeed, residues near the C terminus of helix II (E34, S37, N40-E42) are more exposed in apo-S100A11 than in the calcium form of the protein (Figure 5). This switch in residue packing may be a consequence of the increased exposure of residues in the adjacent linker and helix III that are involved in target protein binding.

In apo-S100A11, helices I and IV are closer to a perpendicular orientation ( $\Omega = 115^\circ$ ) than in the presence of calcium and the annexin peptide ( $\Omega = 127^\circ$ ). The magnitude of this change is nearly twice that observed upon calcium binding to S100B (Drohat et al., 1998; Matsumura et al., 1998; Smith and Shaw, 1998b). Further, a comparison of the changes in the intramolecular I-IV angle with those of helices I-I' (17°) and IV-IV' (0°) reveals it is the movement of helix I that is most responsible. It is possible that a disulfide link between C9 and C9' in the S100A11-annexin I structure (Rety et al., 2000) may contribute to the interactions of helices I and IV. However, C9 is buried in both structures (although not in an oxidized state in apo-S100A11), suggesting a rearrangement of this residue has not occurred (Figure 5).

One result of the reorientation of helices I and IV in apo-S100A11 is a subtle redistribution of side chain exposure of several residues in both helices. Figure 5 shows that the pattern of accessible surface area for apo-S100A11 and S100A11 in complex with calcium and the annexin peptide are different for several residues in these regions. In apo-S100A11, residues P3, I10, E11, I14, and A15 increase their side chain exposure by as much as 25% upon calcium binding. Similarly in helix IV, residues N78, G81, G82, L83, V85, A86, and C87 all increase their side chain exposure to solvent. As will be described, many of these residues are critical for annexin I binding.

The largest structural changes upon calcium binding and target protein interaction involve helices III and IV. This results in extreme changes in side chain surface accessibility (Figure 5) in the calcium binding loop residues for site II (D64-E75). Similarly large changes are noted for site I (A21-E34). The position of helix III changes by approximately 40° with regard to each of helices I, II, and IV. In combination with the helix I-IV and I-I' reorientation, this has the dramatic effect of opening up one face on each side of the apo-S100A11 molecule (Figure 6) and placing helix III nearly perpendicular to helix IV ( $\Omega = 115^\circ$ ) in the calcium-bound structure (Figure 4).

The second most notable feature in apo-S100A11 is the absence of helix between A86 and F101 (Figure 4). Upon calcium (and annexin I) binding, this region becomes helical extending to T95, the third to last residue fitted in the X-ray structure of the complex (Rety et al., 2000). In S100A11, it is not known whether this induction of helix is a result of calcium or peptide binding. However, a similar observation has been made for human and bovine S100B upon calcium binding alone and results in the extension of helix IV by approximately one turn (Matsumura et al., 1998; Smith and Shaw, 1998b). For S100A11, mutational studies have shown

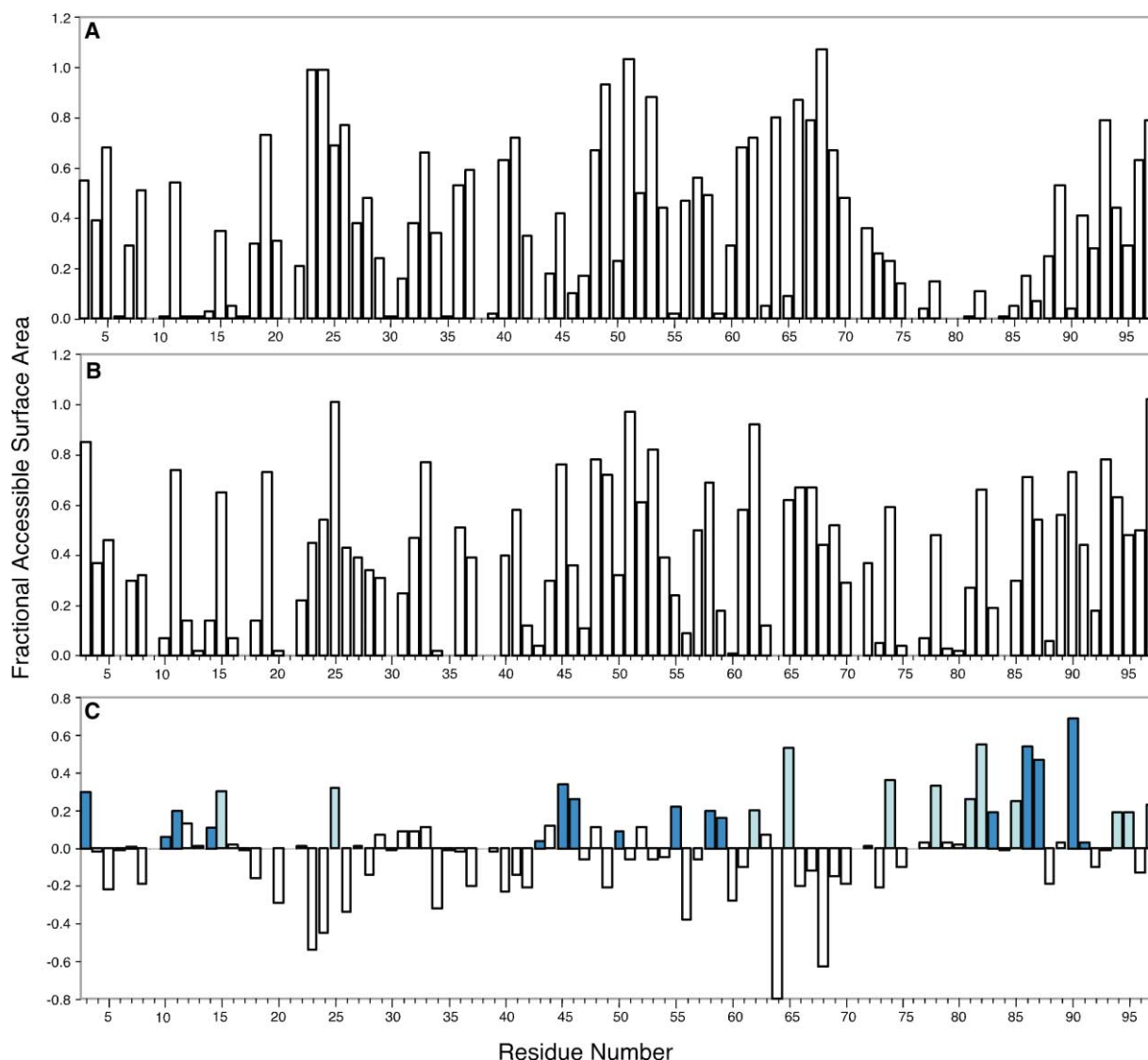


Figure 5. Unmasking of Buried Residues in Apo-S100A11 Important for Annexin I Interactions in the Calcium-Bound S100A11/Annexin I Complex

The fractional accessible surface areas for the side chains of residues in apo-S100A11 (A) and calcium-bound S100A11 (B) (Rety et al., 2000) were calculated from their three-dimensional structures using the program VADAR (University of Alberta). The accessible surface area for the calcium-bound S100A11 complex was determined after removal of the peptide coordinates from the structure. The bottom panel (C) shows the difference in fractional accessible surface area between the two structures and corresponds to the surface area for side chains in apo-S100A11 that become exposed in the calcium-bound annexin I complex. Bars colored dark blue represent residues in S100A11 that have contact ( $<5$  Å) with the annexin I peptide. Many of these increase in side chain exposure by greater than 20% upon calcium binding. Cyan-colored bars represent residues in apo-S100A11 that increase their side chain exposure by  $>20\%$  but do not have direct contact with annexin I in the calcium-bound complex. To facilitate comparison, all sequence numbers correspond to those of rabbit S100A11.

that deletion of residues D91–I94 (E89–V92 in rabbit) dramatically alters the ability of the protein to interact with the N-terminal annexin I peptide upon calcium binding (Seemann et al., 1996). Because these residues are not in a helical structure in apo-S100A11 this would suggest that the conformational change in this region upon calcium binding is important for interaction with annexin I.

#### Specificity for Annexin I Target Interaction

The structure of apo-S100A11 reveals that many residues in helices I, III, and IV and the linker are buried and

less available for interaction with the N-terminal helix in annexin I. Further, several of these residues, important for interaction with annexin I, do not form a contiguous surface required for peptide binding (Figure 6). Specifically, residues P3, I10, E11, S12, I14, and A15 in helix I are more buried in apo-S100A11 than in the S100A11/annexin I complex (Figures 5 and 6). Similar observations are made for helices III and IV where residues V55, R58, and V59, and L83, A86, C87, and S90, respectively, are more buried in apo-S100A11 but have protein-peptide interactions in the complex. These observations clearly indicate that the reorientation of helix III and opening of

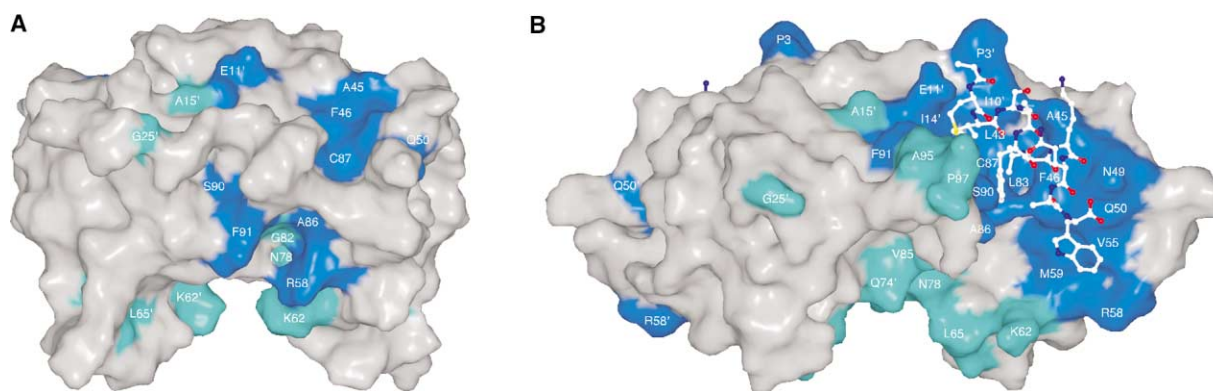


Figure 6. Formation of the Annexin I Binding Surface from Calcium Binding to Apo-S100A11

Accessible surface area representations of apo-S100A11 (A) and calcium-bound S100A11 (B) in complex with annexin I (Rety et al., 2000). Each protein is oriented approximately 90° with respect to that shown in Figure 4. In both molecules, residues in S100A11 that directly interact (<5 Å) with annexin I are indicated and colored dark blue and those whose side chain exposure increases by >20% upon calcium binding but have less interaction are colored cyan. For apo-S100A11 (A), many of these residues have less than 20% of their side chains accessible to the surface and are disjoint on the surface of the protein. In the calcium-bound structure (B), most residues that contact the annexin I peptide increase their side chain-accessible surface areas by >20% as shown in Figure 5C to form a contiguous site for the annexin interaction (dark blue). To facilitate comparison, all sequence numbers correspond to those of rabbit S100A11.

the helix I-IV interaction must occur upon calcium binding to position many of these residues for interaction with the annexin peptide. This results in a stunning transition from a disjointed binding surface in apo-S100A11 to a contiguous surface in the S100A11 complex (Figure 6).

The S100A11-annexin interaction (Rety et al., 2000) is characterized by the bridging of the annexin I peptide with helix I of one monomer and helices III and IV and the linker of the second S100A11 monomer (Figures 4 and 6). Interactions occur between P3 (S100A11; residue numbering refers to the rabbit sequence) and A1 (annexin I), and E11 (S100A11) and A1, M2, and V3 (annexin I), including hydrogen bonds between the E11 side chain carboxylate and M2 and V3 backbone amides. Similar interactions are observed for S100A10-annexin II (Rety et al., 1999) but not for S100B, where interactions between a p53 peptide or TRTK-12 are confined to individual monomers (McClintock and Shaw, 2003; Rustandi et al., 2000). The positions of these residues in the sequences of S100 proteins are among the most variable in S100 proteins. For example, P3 occupies a position that is absent in S100B and S100A12 due to the extended N terminus in S100A11. The position occupied by E11 in S100A11 is conserved in S100A10, S100A11, S100A12, and S100A9, but variable in S100B, S100A5, S100A6, and S100A3. Thus, it would appear that the uncovering of residues P3 and E11 in apo-S100A11 by opening up the helix I-I' interaction (i.e., the interhelical angle) must play an important role for the bridging interactions of annexin I with this region.

In helix IV, residues A86, C87, and S90 increase their exposure upon calcium binding and are required for target interactions (Figures 5 and 6). However, unlike the differences noted in the C terminus of S100A11, these residues are less variable in the S100 sequences. Further, the identical positions in S100B (A83, C84, and F87) possess interactions with the target peptides from TRTK-12 and p53 (McClintock and Shaw, 2003; Rustandi et al., 2000). In S100A11, this region is unstructured in

the apo-protein but is  $\alpha$  helical in the complex, along with F91, which also has contacts with annexin I. Mutagenesis experiments with S100A11 have shown that the region between residues E89 and Q97 is necessary for annexin I binding in the presence of calcium (Seemann et al., 1997). These observations indicate that the induction of helix in the A86–S90 region in apo-S100A11 upon calcium binding is important for target protein interaction. It is interesting that residues H85–F88 become helical upon calcium binding in S100B also (Matsumura et al., 1998; Smith and Shaw, 1998b). However, the similar contacts found for S100B and S100A11 make it difficult to determine how this region confers specificity at present. One difference may occur in the third of these positions where S90 in S100A11 has close contacts (<4 Å) with F6 in annexin I (Figure 6) while F87 has more remote contacts (>5.0 Å) with its bound targets in S100B. Further, it is interesting that S100A11 is one of a handful of S100 proteins (S100A10, S100A3, and S100A4 are others) that has an abnormally long C terminus, 10 and 11 residues longer than S100B and S100A6, respectively. It is possible that induction of  $\alpha$  helix in this region is especially important in these proteins to promote target interactions closer to the protein C terminus. In agreement with this, S100A10, which interacts with annexin II, has been shown to contain numerous contacts from Y85, F86, and M90 near its C terminus (Rety et al., 1999). It might be expected that S100A4 and S100A3 will have this similar feature once structures in complex with calcium and a target protein are obtained.

In the linker of apo-S100A11, residues L43, A44, A45, F46, and D52 are between 50% and 100% buried (Figure 5). In the complex, these residues increase their exposure and have important contacts with the annexin I peptide. The side chain of F46 in S100A11 has contacts with L7 and W11, and A44 is positioned nearby K8 in annexin I. A45 increases its exposure by nearly 40% from that in the apo-state and has contacts with S4, L7, and K8 in annexin I (Figure 6). The sequence of S100A11



in this region of the linker (LAAF) is significantly different from those of S100A10 (FPGF), S100B (LSHF), and S100A6 (LTI—), especially for these central 2 residues. Further, all 4 residues in apo-S100A11 are more buried, become more exposed upon calcium binding and have important contacts with annexin I (Figures 5 and 6). In S100A10, it is the 2 “outside” residues (F38, F41) that interact with residues of annexin II (Rety et al., 1999). In S100B, there are no contacts within 5 Å for residues L40–F43 with either p53 or TRTK-12 targets. In agreement with this, it has been shown that S100A11 does not interact with the S100B target, TRTK-12 (Barber et al., 1999) or the S100A10 target, annexin II (Rety et al., 1999). Further, sequence analysis reveals that residues in the linker region (including LAAF in S100A11) are among the most variable for all S100 sequences. These observations may point to this sequence of residues being important for the specificity of target proteins by individual S100 proteins, although further structural and biological experimentation of other S100 proteins and their targets will be required to support this idea.

### Biological Implications

S100A11 is a member of the S100 protein family of EF-hand calcium binding proteins. The general mechanism for these proteins involves a calcium-induced conformational change allowing them to interact with other target proteins and elicit a biological response. To determine the details of this response, three-dimensional structures of the calcium-free, calcium-bound, and calcium-bound with target protein are required. In this work, the three-dimensional structure of apo-S100A11 has been determined using NMR spectroscopy. The structure reveals that the protein forms a symmetric dimer, with each monomer containing two EF hands. The conformation of site I is similar to that recently determined in calcium-bound S100A11 bound to an annexin I peptide, indicating that calcium binding to this site results in little reorganization. In contrast, helices III and IV, which surround calcium binding site II in apo-S100A11, are near antiparallel, and helices I and IV are more closed than in other S100 proteins. Comparison to the calcium-bound S100A11 structure shows that helix I-IV and I-I' interactions open slightly, while the helix III-IV arrangement is dramatically altered by nearly 40°. Together, these structural changes unmask key residues and provide a contiguous binding surface for annexin I target binding.

One of the proposed biological functions for S100A11 is to aid in the aggregation of membrane surfaces important for cell vesiculation. Annexin I has been shown to interact with phospholipids in a calcium-sensitive manner. Further, interaction between S100A11 and annexin I is dependent on calcium binding to S100A11. Such a calcium-stimulated mechanism would require tight regulation by the calcium binding protein S100A11 in order to time and control membrane aggregation events. The structure of apo-S100A11 reveals that residues important for the interaction with annexin I are hidden from its surface, therefore minimizing the contact between the two proteins. This would allow S100A11 and annexin I to be closely located together near the membrane with little effect on membrane association. Calcium binding

by S100A11 would result in a conformational change that promotes its rapid association with annexin I and stimulation of membrane association.

### Experimental Procedures

#### Sample Preparation

Unlabeled and uniformly  $^{15}\text{N}$ - and  $^{15}\text{N}$ ,  $^{13}\text{C}$ -labeled rabbit S100A11 were expressed in *Escherichia coli* strain BL21(DE3) and purified as previously described (Rintala et al., 2002). Briefly, a 1 L culture was grown at 37°C with agitation to an OD<sub>600</sub> of about 0.7–0.8 and then induced with 0.4 M IPTG for several hours. The cells were harvested by centrifugation, lysed using a French pressure cell, and then subjected to ultracentrifugation at 38,000 rpm and 4°C for 90 min. The supernatant was loaded onto a phenyl-Sepharose column with a calcium-containing buffer and then washed for several hours until the OD<sub>280</sub> returned to baseline. The protein was eluted from the column using the same buffer containing EGTA instead of calcium. Fractions containing the protein were pooled, dialyzed, and lyophilized. Specifically  $^{15}\text{N}$ -glycine/serine-labeled S100A11 was expressed in the auxotrophic cell line, DL39GlyA, and grown on selective medium containing  $^{15}\text{N}$ -glycine as the sole glycine source. Fractionally  $^{13}\text{C}$ -labeled S100A11 was prepared by growing BL21(DE3) on M9 minimal medium containing a 1:10 mixture of fully  $^{13}\text{C}$ -labeled glucose and unlabeled glucose, respectively (Neri et al., 1989). Asymmetrically labeled S100A11 was prepared by incubating a 1:1 mixture of unlabeled S100A11 (36 μM) and  $^{13}\text{C}$ ,  $^{15}\text{N}$ -labeled S100A11 (36 μM) in 50 ml of water for approximately 220 hr in the presence of 0.2 mM dithiothreitol at 37°C with agitation. The progression of the reaction was monitored by electrospray mass spectrometry under nondenaturing conditions. The protein solution was lyophilized and then dissolved in 5 ml of 100% D<sub>2</sub>O and incubated overnight and then repeated. The solution was concentrated to 600 μl with a final monomer concentration of 3 mM of each protein, deuterated dithiothreitol was added to a concentration of 10 mM, and the pH was adjusted to 7.25. All other NMR samples were prepared at a dimer concentration of 1 mM in 90% H<sub>2</sub>O/10% D<sub>2</sub>O (v/v), 50 mM KCl, 10 mM dithiothreitol (pH 7.25).

#### NMR Spectroscopy

NMR experiments were performed at 35°C on Varian 500, 600, and 800 MHz spectrometers with pulse field gradient triple-resonance probes. Sequential assignments of the polypeptide backbone resonances for apo-S100A11 were made from HNCA, HN(CO)CA, HNCACB, CBCA(CO)NH (Grzesiek and Bax, 1992), and  $^1\text{H}$ - $^{15}\text{N}$  HSQC experiments (Kay et al., 1992). Side chain resonance assignments were made from  $^{15}\text{N}$ -edited TOCSY, C(CO)NH, HCCH-TOCSY (Kay et al., 1993), HC(CO)NH, HBCBCGCDHD, HBCBCGCDCEHE (Yamazaki et al., 1993), and  $^1\text{H}$ - $^{13}\text{C}$  HSQC experiments. The  $^1\text{H}$ ,  $^{13}\text{C}$ , and  $^{15}\text{N}$  resonances of apo-S100A11 have been assigned and deposited in the BioMagResBank under accession number BMRB-5189. Fractionally  $^{13}\text{C}$ -labeled S100A11 protein was used to collect  $^{13}\text{C}$ -coupled and decoupled  $^1\text{H}$ - $^{13}\text{C}$  HSQC spectra in order to stereo-specifically assign prochiral methyl groups for valine and leucine residues. The  $^{13}\text{C}$ -coupled  $^1\text{H}$ - $^{13}\text{C}$  HSQC was collected using 512 increments in order to be able to observe the splitting in the  $^{13}\text{C}$  dimension. Amide exchange was determined by dissolving S100A11 protein in 100% D<sub>2</sub>O and collecting a  $^1\text{H}$ - $^{15}\text{N}$  HSQC spectrum after a 10 hr incubation. Interproton distances were obtained from  $^{15}\text{N}$ -NOESY and  $^{13}\text{C}$ ,  $^{15}\text{N}$ -NOESY spectra. The  $^{15}\text{N}$ -NOESY spectrum was collected on a Varian 600 MHz spectrometer with a 150 ms mixing time. The  $^{13}\text{C}$ ,  $^{15}\text{N}$ -NOESY spectrum (Pascal et al., 1994) was collected on an INOVA 800 MHz spectrometer with a 100 ms mixing time. A  $^{13}\text{C}$  F<sub>1</sub>-filtered, F<sub>3</sub>-edited NOESY experiment (Zwahlen et al., 1997) was collected on an INOVA 800 MHz spectrometer with a 150 ms mixing time.

#### Structure Determination

Structures of apo-S100A11 were calculated using the simulated annealing protocol in the CNS program (Brunger et al., 1998). Dimeric S100A11 structures were generated using a total of 2964 nOes, including 1336 intraresidue, 658 sequential, 594 short-range,

264 long-range, and 112 intermonomer distances as well as 64 hydrogen bond distance restraints and 192 dihedral restraints. Interproton distances for all proton pairs, except intermonomer nOes, were calibrated using maximum and minimum nOe intensities for known possible  $d_{NH\alpha}$  distances. Dihedral angle restraints were determined by the TALOS (torsion angle likelihood obtained from shifts and sequence similarity) program (Cornilescu et al., 1999) based on chemical shift data from the  $H_{\alpha}$ ,  $C_{\alpha}$ ,  $C_{\beta}$ , and CO resonances of apo-S100A11 and sequence similarity. Angles were selected when nine of ten dihedral matches fell within an allowed region of the Ramachandran plot. These angles were restricted to  $\psi \pm \text{error}^{\circ}$  and  $\phi \pm \text{error}^{\circ}$  for structure calculations where the error was the deviation from the average angle selected by TALOS. Hydrogen bonds were identified from slowly exchanging NH resonances after a 10 hr incubation of apo-S100A11 in  $D_2O$ . For each hydrogen bond, two distance restraints were used, NH-O (1.8–2.3 Å) and N-O (2.3–3.3 Å). Structure determination of the apo-S100A11 dimer involved the use of noncrystallographic symmetry. Intermonomer distance restraints were not calibrated and were set to maximum and minimum distances of 6.00 and 1.70 Å, respectively, for all calculations.

#### Acknowledgments

The authors would like to thank Kathryn Barber (UWO) for her excellent technical support, Frank Delaglio and Dan Garrett (NIH) for the programs NMRPipe and Pipp, Lewis Kay (University of Toronto) for all pulse sequences, and Brett Schönekeß (University of Calgary) for the S100A11 cDNA used in this work. We would like to thank the Canadian National High Field NMR Centre (NANUC, Edmonton, Alberta) for acquisition of the  $^{13}C$  F<sub>1</sub>-edited, F<sub>3</sub>-filtered NOESY-HSQC experiment and Dr. L. Spyropoulos (University of Alberta) for helpful discussions. This research was supported from operating and maintenance grants from the Canadian Institutes of Health Research (GSS) and graduate studentships from the Natural Sciences and Engineering Research Council and Canadian Institutes of Health Research (A.C.D.). M.P.W. is an Alberta Heritage Foundation for Medical Research Scientist and a recipient of a Canada Research Chair (Tier I) in Biochemistry. The 600 MHz NMR spectrometer at UWO was funded through grants from the Canada Foundation for Innovation, Ontario Innovation Trust, and the Academic Development Fund of The University of Western Ontario. Operation of NANUC is funded by the Canadian Institutes of Health Research, the Natural Sciences and Engineering Research Council of Canada, and the University of Alberta.

Received: January 31, 2003

Revised: April 4, 2003

Accepted: April 18, 2003

Published: July 1, 2003

#### References

Akke, M., Drakenberg, T., and Chazin, W. (1992). Three-dimensional solution structure of  $Ca^{2+}$  loaded porcine calbindin  $D_{9k}$  determined by nuclear magnetic resonance spectroscopy. *Biochemistry* 31, 1011–1020.

Allen, B.G., Durussel, I., Walsh, M.P., and Cox, J.A. (1996). Characterization of the  $Ca^{2+}$ -binding properties of calgizzarin (S100C) isolated from chicken gizzard smooth muscle. *Biochem. Cell Biol.* 74, 687–694.

Barber, K.R., McClintock, K.A., Jamieson, G.A., Jr., Dimlich, R.V., and Shaw, G.S. (1999). Specificity and  $Zn^{2+}$  enhancement of the S100B binding epitope TRTK-12. *J. Biol. Chem.* 274, 1502–1508.

Baudier, J., Delphin, C., Grunwald, D., Khochbin, S., and Lawrence, J.J. (1992). Characterization of the tumor suppressor protein p53 as a protein kinase C substrate and a S100b-binding protein. *Proc. Natl. Acad. Sci. USA* 89, 11627–11631.

Becker, T., Gerke, V., Kube, E., and Weber, K. (1992). S100P, a novel  $Ca^{2+}$ -binding protein from human placenta: cDNA cloning, recombinant protein expression and  $Ca^{2+}$  binding properties. *Eur. J. Biochem.* 207, 541–547.

Bianchi, R., Pula, G., Ceccarelli, P., Giambanco, I., and Donato, R.

(1992). S-100 protein binds to annexin II and p11, the heavy and light chains of calpactin I. *Biochim. Biophys. Acta* 1160, 67–75.

Brunger, A.T., Adams, P.D., Clore, G.M., DeLano, W.L., Gros, P., Grosse-Kunstleve, R.W., Jiang, J.-S., Kunzowski, J., Nilges, M., Pannu, N.S., et al. (1998). Crystallography & NMR system: a new software suite for macromolecular structure determination. *Acta Crystallogr. D* 54, 905–921.

Cornilescu, G., Delaglio, F., and Bax, A. (1999). Protein backbone angle restraints from searching a database for chemical shift and sequence homology. *J. Biomol. NMR* 13, 289–302.

Delphin, C., Ronjat, M., Deloulme, J.C., Garin, G., Debussche, L., Higashimoto, Y., Sakaguchi, K., and Baudier, J. (1999). Calcium-dependent interaction of S100B with the C-terminal domain of the tumor suppressor p53. *J. Biol. Chem.* 274, 10539–10544.

Donato, R. (2001). S100: a multigenic family of calcium-modulated proteins of the EF-hand type with intracellular and extracellular functional roles. *Int. J. Biochem. Cell Biol.* 33, 637–668.

Drohat, A.C., Baldisseri, D.M., Rustandi, R.R., and Weber, D.J. (1998). Solution structure of calcium-bound rat S100B ( $\beta\beta$ ) as determined by nuclear magnetic resonance spectroscopy. *Biochemistry* 37, 2729–2740.

Drohat, A.C., Tjandra, N., Baldisseri, D.M., and Weber, D.J. (1999). The use of dipolar couplings for determining the solution structure of rat apo-S100B( $\beta\beta$ ). *Protein Sci.* 8, 800–809.

Fritz, G., Mittl, P.R.E., Vasak, M., Grutters, M.G., and Heizmann, C.W. (2002). The crystal structure of metal-free human EF-hand protein S100A3 at 1.7 Å resolution. *J. Biol. Chem.* 277, 33092–33098.

Fujii, T., Machino, K., Andoh, H., Satoh, T., and Kondo, Y. (1990). Calcium-dependent control of caldesmon-actin interaction by S100 protein. *Biochemistry* 107, 133–137.

Garbuglia, M., Verzini, M., and Donato, R. (1998). Annexin VI binds S100A1 and S100B and blocks the ability of S100A1 and S100B to inhibit desmin and GFAP assemblies into intermediate filaments. *Cell Calcium* 24, 177–191.

Garbuglia, M., Verzini, M., Rustandi, R.R., Osterloh, D., Weber, D.J., Gerke, V., and Donato, R. (1999). Role of the C-terminal extension in the interaction of S100A1 with GFAP, tubulin, the S100A1- and S100B-inhibitory peptide, TRTK-12, and a peptide derived from p53, and the S100A1 inhibitory effect on GFAP polymerization. *Biochem. Biophys. Res. Commun.* 254, 36–41.

Gerke, V. (1990). Tyrosine kinase substrate annexin II (p36)—biochemical characterization and conservation among species. *Biochem. Soc. Trans.* 18, 1106–1108.

Gerke, V., and Moss, S.E. (2002). Annexins: from structure to function. *Physiol. Rev.* 82, 331–371.

Grzesiek, S., and Bax, A. (1992). An efficient experiment for sequential backbone assignment of medium-sized isotopically enriched proteins. *J. Magn. Reson.* 99, 201–207.

Heizmann, C.W. (1999).  $Ca^{2+}$ -binding S100 proteins in the central nervous system. *Neurochem. Res.* 24, 1097–1100.

Heizmann, C.W., Fritz, G., and Schafer, B.W. (2002). S100 proteins: structure, functions and pathology. *Front. Biosci.* 7, d1356–d1368.

Ikura, M. (1996). Calcium binding and conformational response in EF-hand proteins. *Trends Biochem. Sci.* 21, 14–17.

Ikura, M., Clore, G.M., Gronenborn, A.M., Zhu, G., Klee, C.B., and Bax, A. (1992). Solution structure of a calmodulin-target peptide complex by multidimensional NMR. *Science* 256, 632–638.

Kay, L.E., Keifer, P., and Saarinen, T. (1992). Pure absorption gradient enhanced heteronuclear single quantum correlation spectroscopy with improved sensitivity. *J. Am. Chem. Soc.* 114, 10663–10665.

Kay, L.E., Xu, G., Singer, A.U., Muhandiram, D.R., and Forman-Kay, J.D. (1993). A gradient-enhanced HCCH-TOCSY experiment for recording side-chain  $^1H$  and  $^{13}C$  correlations in  $H_2O$  samples of proteins. *J. Magn. Reson.* 101, 333–337.

Kilby, P.M., Van Eldik, L.J., and Roberts, G.C.K. (1996). The solution structure of the bovine S100b protein dimer in the calcium-free state. *Structure* 4, 1041–1052.

- Kordel, J., Skelton, N.J., Akke, M., and Chazin, W.J. (1993). High resolution solution structure of calcium-loaded calbindin D<sub>9k</sub>. *J. Mol. Biol.* 231, 711–734.
- Maler, L., Potts, B.C., and Chazin, W.J. (1999). High resolution solution structure of apo calyculin and structural variations in the S100 family of calcium-binding proteins. *J. Biomol. NMR* 13, 233–247.
- Maler, L., Sastry, M., and Chazin, W.J. (2002). A structural basis for S100 protein specificity derived from comparative analysis of apo and Ca<sup>2+</sup>-calyculin. *J. Mol. Biol.* 317, 279–290.
- Martin, S.R., Bayley, P.M., Brown, S.E., Porumb, S.E., Zhang, M., and Ikura, M. (1996). Spectroscopic characterization of a high-affinity calmodulin-target peptide hybrid molecule. *Biochemistry* 35, 3508–3517.
- Matsumura, H., Shiba, T., Inoue, T., Harada, S., and Kai, Y. (1998). A novel mode of target recognition suggested by the 2.0 Å structure of holo S100B from bovine brain. *Structure* 6, 233–241.
- McClintock, K.A., and Shaw, G.S. (2003). A novel S100 target conformation is revealed by the solution structure of the Ca<sup>2+</sup>-S100B-TRTK-12 complex. *J. Biol. Chem.* 278, 6251–6257.
- McKay, R.T., Tripet, B.P., Hodges, R.S., and Sykes, B.D. (1997). Interaction of the second binding region of troponin I with the regulatory domain of skeletal muscle troponin C as determined by NMR spectroscopy. *J. Biol. Chem.* 272, 28494–28500.
- Neri, D., Szyperski, T., Otting, G., Senn, H., and Wuthrich, K. (1989). Stereospecific nuclear magnetic resonance assignments of the methyl groups of valine and leucine in the DNA-binding domain of the 434 repressor by biosynthetically directed fractional <sup>13</sup>C labeling. *Biochemistry* 28, 7510–7516.
- Odink, K., Cerletti, N., Bruggen, J., Clerc, R.G., Tarcsay, L., Zwadlo, G., Gerhards, G., Schlegel, R., and Sorg, C. (1987). Two calcium-binding proteins in infiltrate macrophages of rheumatoid arthritis. *Nature* 330, 80–82.
- Olwin, B.B., and Storm, D.R. (1985). Calcium binding to complexes of calmodulin and calmodulin binding proteins. *Biochemistry* 24, 8081–8086.
- Otterbein, L.R., Kordowska, J., Witte-Hoffmann, C., Wang, C.L.A., and Dominguez, R. (2002). Crystal structures of S100A6 in the Ca<sup>2+</sup>-free and Ca<sup>2+</sup>-bound states: the calcium sensor mechanism of S100 proteins revealed at atomic resolution. *Structure* 10, 557–567.
- Pascal, S.M., Muhandiram, D.R., Yamazaki, T., Forman-Kay, J.D., and Kay, L.E. (1994). Simultaneous acquisition of <sup>15</sup>N- and <sup>13</sup>C-edited NOE spectra of protein dissolved in H<sub>2</sub>O. *J. Magn. Reson. B* 103, 197–201.
- Petrova, T.V., Hu, J., and Van Eldik, L.J. (2000). Modulation of glial activation by astrocyte-derived protein S100B: differential responses of astrocyte and microglial cultures. *Brain Res.* 853, 74–80.
- Potts, B.C.M., Smith, J., Akke, M., Macke, T.J., Okazaki, K., Hidaka, H., Case, D.A., and Chazin, W.J. (1995). The structure of calyculin reveals a novel homodimeric fold for S100 Ca<sup>2+</sup>-binding proteins. *Nat. Struct. Biol.* 2, 790–796.
- Rety, S., Sopkova, J., Renouard, M., Osterloh, D., Gerke, V., Tabaries, S., Russo-Marie, R., and Lewit-Bentley, A. (1999). The crystal structure of a complex of p11 with the annexin II N-terminal peptide. *Nat. Struct. Biol.* 6, 89–95.
- Rety, S., Osterloh, D., Arie, J.-P., Tabaries, S., Seemann, J., Russo-Marie, F., Gerke, V., and Lewit-Bentley, A. (2000). Structural basis of the Ca<sup>2+</sup>-dependent association between S100C (S100A11) and its target, the N-terminal part of annexin I. *Structure* 8, 175–184.
- Rintala, A.C., Schönekeess, B.O., Walsh, M.P., and Shaw, G.S. (2002). <sup>1</sup>H, <sup>15</sup>N and <sup>13</sup>C resonance assignments of rabbit apo-S100A11. *J. Biomol. NMR* 22, 191–192.
- Rustandi, R.R., Baldisseri, D.M., and Weber, D.J. (2000). Structure of the negative regulatory domain of p53 bound to S100B. *Nat. Struct. Biol.* 7, 570–574.
- Rustandi, R.R., Baldisseri, D.M., Inman, K.G., Nizner, P., Hamilton, S.M., Landar, A., Zimmer, D.B., and Weber, D.J. (2002). Three-dimensional solution structure of the calcium-signaling protein apo-S100A1 as determined by NMR. *Biochemistry* 41, 788–796.
- Sastry, M., Ketchem, R.R., Crescenzi, O., Weber, C., Lubienski, M.J., Hidaka, H., and Chazin, W.J. (1998). The three-dimensional structure of Ca<sup>2+</sup>-bound calyculin: implications for Ca<sup>2+</sup>-signal transduction by S100 proteins. *Structure* 6, 223–231.
- Schönekeess, B.O., and Walsh, M.P. (1997). Molecular cloning and expression of avian smooth muscle S100A11 (calgizzarin, S100C). *Biochem. Cell Biol.* 75, 771–775.
- Seemann, J., Weber, K., and Gerke, V. (1996). Structural requirements for annexin I-S100C complex formation. *Biochem. J.* 319, 123–129.
- Seemann, J., Weber, K., and Gerke, V. (1997). Annexin I targets S100C to early endosomes. *FEBS Lett.* 413, 185–190.
- Skelton, N.J., Kordel, J., and Chazin, W.J. (1995). Determination of the solution structure of apo calbindin D<sub>9k</sub> by NMR spectroscopy. *J. Mol. Biol.* 249, 441–462.
- Smith, S.P., and Shaw, G.S. (1998a). A change-in-hand mechanism for S100 signalling. *Biochem. Cell Biol.* 76, 324–333.
- Smith, S.P., and Shaw, G.S. (1998b). A novel calcium-sensitive switch revealed by the structure of human S100B in the calcium-bound form. *Structure* 6, 211–222.
- Vallely, K.M., Rustandi, R.R., Ellis, K.C., Varlamova, O., Bresnick, A.R., and Weber, D.J. (2002). Solution structure of human Mts1 (S100A4) as determined by NMR spectroscopy. *Biochemistry* 41, 12670–12680.
- Van Eldik, L.J., and Griffin, W.S.T. (1994). S100b expression in Alzheimer's disease: relation to neuropathology in brain regions. *Biochim. Biophys. Acta* 1223, 398–403.
- Wimberly, B., Thulin, E., and Chazin, W.J. (1995). Characterization of the N-terminal half-saturated state of calbindin D9k: NMR studies of the N56A mutant. *Protein Sci.* 4, 1045–1055.
- Yamazaki, T., Forman-Kay, J.D., and Kay, L.E. (1993). Two-dimensional NMR experiments for correlating <sup>13</sup>Cβ and <sup>1</sup>Hδ/ε chemical shifts of aromatic residues in <sup>13</sup>C-labeled proteins via scalar couplings. *J. Am. Chem. Soc.* 115, 11054–11055.
- Yazawa, M., Ikura, M., Hikichi, K., Ying, L., and Yagi, K. (1987). Communication between two globular domains of calmodulin in the presence of mastoparan or caldesmon fragment. Ca<sup>2+</sup> and <sup>1</sup>H NMR. *J. Biol. Chem.* 262, 10951–10954.
- Zhao, X.Q., Naka, M., Muneyuki, M., and Tanaka, T. (2000). Ca<sup>2+</sup>-dependent inhibition of actin-activated myosin ATPase activity by S100C (S100A11), a novel member of the S100 protein family. *Biochem. Biophys. Res. Commun.* 267, 77–79.
- Zwahlen, C., Legault, P., Vincent, S.J.F., Greenblatt, J., Konrat, R., and Kay, L.E. (1997). Methods for measurement of intermolecular NOEs by multinuclear NMR spectroscopy: application to a bacteriophage λ N-peptide/boxB RNA complex. *J. Am. Chem. Soc.* 119, 6711–6721.

## Accession Numbers

The coordinates for apo-S100A11 have been deposited in the Protein Data Bank under ID code 1NSH.